# STUDIES OF PHOTOREDOX REACTIONS ON NANOSIZE SEMICONDUCTORS



Jess P. Wilcoxon, Sandia National Laboratories, Org 1152, Albuquerque, NM; F. Parsapour, D.F. Kelley, Colorado State U., Dept. of Chemistry, Fort Collins, Co.



## ABSTRACT

Light induced electron transfer (ET) from nanosize semiconductors of $MoS_2$ to organic electron acceptors such as 2,2'-bipyridine (bpy) and methyl substituted 4,4',5,5'-tetramethyl-2,2'-bipyridine (tmb) was studied by static and time resolved photoluminescence spectroscopy. The kinetics of ET were varied by changing the nanocluster size (the band gap), the electron acceptor, and the polarity of the solvent. $MoS_2$ is an especially interesting semiconductor material as it is an indirect semiconductor in bulk form, and has a layered covalent bonding arrangement which is highly resistant to photocorrosion.



## INTRODUCTION

$MoS_2$ is an especially interesting semiconductor material as it is an indirect semiconductor in bulk form and has a layered covalent bonding arrangement, which resists photocorrosion. Its most common industrial applications include thermal catalysis to remove sulfur compounds from crude oil and as an excellent high temperature lubricant (e.g. axle grease). In fact, in bulk form $MoS_2$ in the most widely used hydrotreating catalyst and thus is vital to all chemical processing for fuels and feedstocks.

However, because $MoS_2$ is an indirect gap, black, IR absorbing material, it has no application as a photocatalyst. We have demonstrated that when synthesized in nanosize form, the absorption edge of $MoS_2$ can be significantly blue shifted.[1] This increase in the band gap energy, due to quantum confinement, is accompanied by significant shifts in both conduction and valence band energies, and implies that nanosize $MoS_2$ is capable of light induced electron and hole transfer (photoredox) reactions, just as are well known direct gap materials such as CdS. Experimentally, there is evidence that as $MoS_2$ is made smaller, the excitation becomes more like a direct transition, presumably due to the increasing importance of surface and lack of long-range translational symmetry in the lattice.

In this paper we report on static and dynamic photoluminesence measurements of nanosize $MoS_2$ and show that the observed increases in the bandgap energy with decreasing nanocluster size, are accompanied by increases in the conductance band potential which permit electron transfer ~~electron~~ to acceptor organic molecules. The rate of electron transfer is found to be dependent on both nanocluster size and solvent polarity. The fastest rates are observed in solvents of high polarity.



## EXPERIMENT

### Synthesis, Processing, and Physical Characterization

Nanosize $MoS_2$ is prepared by dissolving an anhydrous $MoX_4$ salt (X=Cl, Br, or I) in a water and air-free inverse micelle solution. (A typical inverse micelle solution would consist of 5-10% by weight of a quaternary ammonium surfactant in an aliphatic hydrocarbon such as octane).[2] This precursor solution is then exposed to a source of sulfide, typically $H_2S$ gas injected through a septum in a known amount (slightly greater than 2:1 S:Mo) while rapidly stirring the solution. A brightly colored, transparent solution is formed which is then purified by extraction into an oil-immisible phase solvent, typically acetonitrile (ACN). Alternatively, we have developed high pressure liquid chromatographic (HPLC) procedures to both separate the nanoclusters from the surfactants and ionic byproducts in the solution and optically characterize

# DISCLAIMER

the purified nanoclusters on-line.[3] Gas-Chromatography/Mass Spectrometry is used to ascertain that the organic byproducts have been removed from the reaction mixture.

The purified $MoS_2$ clusters have been investigated using HRTEM and shown to be nanocrystalline. The larger nanoclusters have been shown to have the bulk hexagonal lattice structure by electron diffraction, but the smallest clusters (diameter, D<3 nm) have too few atoms to give unambiguous structural information based upon diffraction. However, lattice fringe images are consistent with d spacings found in the bulk material. Evidence indicates that the clusters are not spherical in shape, but are disc-like. The sandwich-like structure of $MoS_2$ consists of successive S-Mo-S tri-layers, with a weak Van-der-Waals interaction between layers. This graphite-like structure is responsible for the good lubricating properties of bulk $MoS_2$, since these planes can readily slide past one another.

Dynamic light scattering is complementary to measurements of cluster cross-sectional size by TEM since it measures the translational diffusion of the cluster in the acetonitrile solution, and via Stokes law provides an equivalent sphere hydrodynamic diameter. This diameter is comparable to the cross-sectional area for nanoclusters with D~3.0 nm, but is smaller for the D~4.5 nm clusters, implying the thickness of the latter clusters is somewhat less than the cross-sectional TEM measurement.

## $MoS_2$ Optical Properties and Electronic Structure

Bulk $MoS_2$ is an indirect band-gap semiconductor, with a band gap of 1.23 eV.[4] As in the case of other indirect materials such as Si and Ge, no room temperature photoluminesence can be observed. Studies of thin crystalline films of $MoS_2$ reveal that the first direct absorbance in $MoS_2$ occurs at 1.88 eV, corresponding to ~660 nm. In bulk form, the top of the valence band is composed primarily of Mo $d_{z^2}$ orbitals, and the bottom of the conduction band is composed of Mo $D_{x^2-y^2}$ and $d_{xy}$ orbitals. As a result, excitation to create hole-electron pairs is metal intraband in nature and no Mo-S bonds are weakened, giving this material strong resistance to photocorrosion.[5] In contrast, II-IV semiconductors such as CdS have valence band orbitals consisting mainly of S 3p states, so that direct excitation across the gap to conduction band Cd 5s states leads to weakening of the chemical bonds holding the material together and accounts for the observed significant photocorrosion in these semiconductors.

As $MoS_2$ is made smaller, the momentum selection rules due to the long-range translational symmetry of the lattice are relaxed. In effect, the material becomes more like a direct band-gap material. As shown in figures 1 and 2 this results in increased room temperature photoluminesence and larger optical extinction in the visible absorbance. (The extinction coefficients can be obtained from these figures by multiplying by 1000 since the $[MoS_2] \sim 1 \times 10^{-3}$M, and are in the $10^4$ to $10^5$ $cm^{-1}$-$mol^{-1}$ range)

A significant portion of the observed luminesence occurs to the red of the absorbance band-edge indicating that recombination is occurring primarily from sub-band-gap trapped states at the surface of the nanocluster. Addition of an electron acceptor such as bipyridine, bpy to the $MoS_2$ nanocluster will decrease the lifetime of these deep trap states by funneling some of the electrons created by direct excitation to the electron acceptor bpy, from which recombination with the hole on the $MoS_2$ nanocluster will also occur. This allows us to follow the electron transfer kinetic indirectly. A more direct alternative approach to following the ET kinetics involves measurement of the change in the bpy absorbance due to ET as a function of time. We are currently pursuing such studies.

An obvious result of making smaller $MoS_2$ nanoparticles is the blue shift of the absorbance edge shown in figures 1 and 2, a corresponding blue shift of the emission, and an increased quantum efficiency for luminesence.

We can roughly estimate the conduction and valence band energies of our nanosize $MoS_2$ clusters by using the known potentials of the bulk material of +0.1 V and +1.33 V (vs. NHE) respectively. If we attribute most the band-gap shift observed in figure 1 and 2 to changes in the conduction band potential (because of the lower electron compared to hole mass) then we estimate a value of -.66 V and -1.46 V vs. NHE for the D=4.5 nm and D=3.0 nm samples.[6]

By photoexciting at the direct point we produce conduction band electrons with about 0.25 eV higher energies (more negative potential) than the above values. So nanoclusters will have a significant driving force for electron transfer compared to the bulk material.

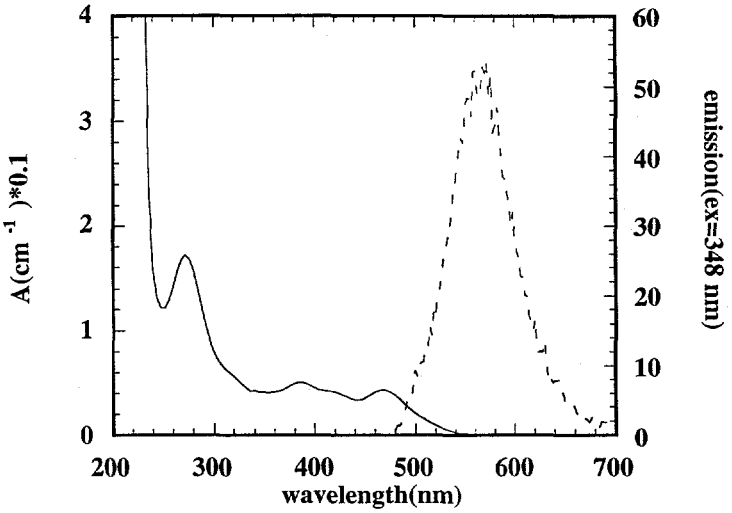


Figure 1. Absorbance (solid curve), and photoluminesence (dashed curve) from D=4.5 nm $MoS_2$ nanoclusters.

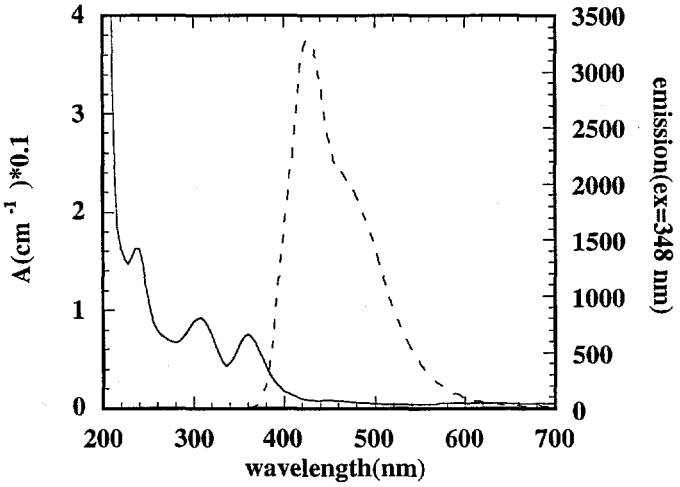


Figure 2. Absorbance (solid curve), and photoluminesence (dashed curve) from D=3.0 nm $MoS_2$ nanoclusters.

Static PL Quantum Efficiency

Table I summarizes the results of PL integrated area, PL(area), normalized by the cluster absorbance (abs) at the excitation wavelength indicated for one size, D=3.0 nm of nanocluster. Very similar trends were observed for other sizes of cluster. Also shown in this table are the results for Coumarin 500 dye (nearly 100% Q.E. for PL) under identical instrumental conditions. We note the very significant decrease in radiative recombination (PL) as the solvent polarity decreases from ethylene glycol to o-xylene. This effect is greatest for excitation at the first direct absorbance (~340 nm, see figure 2) compared to excitation at the band edge (~400 nm). Furthermore, we observe an interesting *decrease* in PL by 5-fold when bpy is bound to the nanocluster and excitation is at 340 nm. Band edge excitation, on the other hand, actually *increases* the yield by ~15% when bpy is bound. Additionally, changing the solvent can alter the overall wavelength dependence of the PL for excitation at the first absorbance feature. (There is little effect for excitation at the band edge) Basically, solvating the clusters in very non-polar

solvents such as toluene increases the amount of light emitted from trapped surface states, effectively red-shifting the PL peak by ~20 nm compared to polar solvents such as ethylene glycol.

Table I. Effect of Solvent Polarity on PL Quantum Efficiency for $MoS_2$ nanoclusters

| Size(nm) | solvent | λ(excit) | <λ(emis)> | PL(area)/abs |
|---|---|---|---|---|
| Coumarin 500 | methanol | 350 | 497 | $1.5 \times 10^{10}$ |
| 3.0 | Ethylene Glycol | 350 | 465 | $1.0 \times 10^{7}$ |
| 3.0 | DMF | 340 | 481 | $5.8 \times 10^{4}$ |
| 3.0 | acn | 340 | 456 | $2.2 \times 10^{5}$ |
| 3.0 | acn/bpy | 340 | 461 | $4.1 \times 10^{4}$ |
| 3.0 | hexanol | 340 | 462 | $5.9 \times 10^{5}$ |
| 3.0 | octanol | 340 | 460 | $4.2 \times 10^{5}$ |
| 3.0 | toluene | 340 | 482 | $2.1 \times 10^{4}$ |
| 3.0 | o-xylene | 340 | 483 | $8.4 \times 10^{3}$ |
| Coumarin 500 | methanol | 400 | 496 | $2.1 \times 10^{10}$ |
| 3.0 | Ethylene Glycol | 400 | 485 | $1.9 \times 10^{7}$ |
| 3.0 | dmf | 400 | 485 | $2.5 \times 10^{6}$ |
| 3.0 | acn | 400 | 484 | $1.3 \times 10^{7}$ |
| 3.0 | acn/bpy | 400 | 480 | $1.5 \times 10^{7}$ |
| 3.0 | hexanol | 400 | 478 | $7.0 \times 10^{6}$ |
| 3.0 | octanol | 400 | 479 | $6.1 \times 10^{6}$ |
| 3.0 | toluene | 400 | 486 | $8.2 \times 10^{5}$ |
| 3.0 | o-xylene | 400 | 481 | $2.1 \times 10^{5}$ |

ET Studies

The layer-like structure of both bulk and nanosize $MoS_2$ has important implications for its use as a photocatalyst. The basal planes of sulfur atoms are relatively inert and bifunctional electron donating ligands such as bipyridine (bpy) (used in the present study) will bind to the Mo at edge sites of the disc-like $MoS_2$ nanoclusters. Such binding can be demonstrated to be quite strong as a $MoS_2$/bpy complex elutes as a single entity during HPLC.[6] It has been further demonstrated that the molar ratio of Mo to bpy at full edge site occupation is about 2:1, and so this was the chosen concentration for bpy, and tetramethyl substituted bpy (tmb) used in our studies.

The actual reduction potentials of bpy and tmb are quite sensitive to the type of metal to which they are bound and the chemical environment (solvent polarity etc.). Never-the-less, the difference of potential of 0.29 V between the two acceptors (tmb, is more difficult to reduce), remains quite constant. So, by adding these electron acceptors to the two different sized $MoS_2$ nanocluster samples and observing the changes in the PL decay curves shown in figure 3 and 4, one can estimate this potential. All PL relaxations were obtained with 315 nm excitation while detection was at 420 nm for the D=3.0 nm sample and 560 nm for the D=4.5 nm sample. The decay times do depend on the detected wavelength somewhat. Addition of tmb to the $MoS_2$, D=4.5 nm sample results in a very small change in the PL decay curve of figure 4., and we conclude that the potentials of tmb and bpy for reduction in acetonitrile are ~-0.7 V and -.41 V vs. NHE respectively. (The decay curve of bound tmb overlaps the bare nanocluster curve of figure 4 and so is not shown).

Since the decay curves obtained are very non-exponential and represent a very wide range of decay rates, one can obtain excellent fits to these data by using a stretched exponential form, $Ae^{-(\Gamma t)^{\beta}}$ from which the decay rate $\Gamma$ can be extracted. A complicating factor is that the stretched

exponential exponent β changes along with Γ when bpy is bound to the cluster, as well as when different solvents are used. This implies that the various mechanisms for radiative recombination for a given size cluster are influenced by the details of the cluster interface. Complete details for such energy calculations and the underlying assumptions are given elsewhere [6].

From analysis of the blue shifts of the absorbance spectra and our ET kinetics for nanosize $MoS_2$, we have estimated the conduction band potential of the D=3.0 and D=4.5 nm nanoclusters to be -1.71 V and -0.91 V, respectively, in acetonitrile.[6] If we recall the estimated potential in the bulk material is +0.1 V, we can see that quantum size effects have made these nanoclusters into very strong reducing agents.

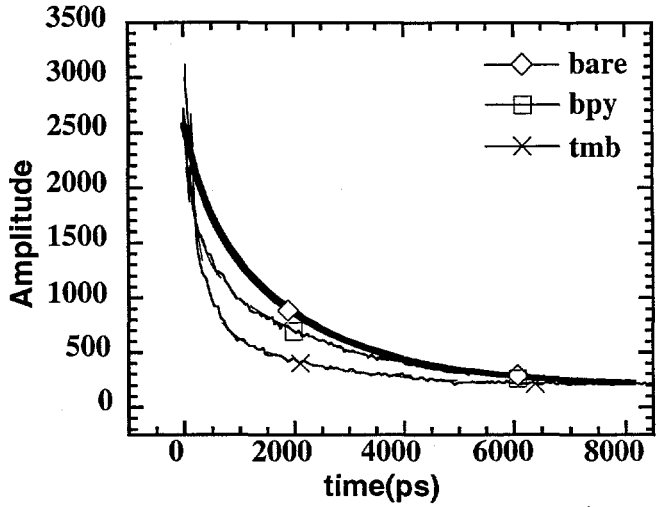


Figure 3. The decay of the photoluminesence of D=3.0 nm $MoS_2$ nanoclusters for various electron acceptors added.

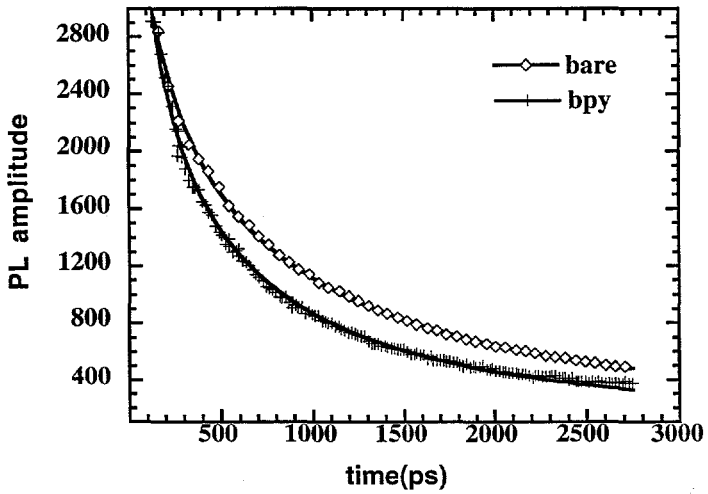


Figure 4. The decay of the photoluminesence of bare, D=4.5 nm $MoS_2$ nanoclusters and $MoS_2$ with bpy.

Size Dependence

Some of the results of our studies on ET kinetics are summarized in figure 5. We first note that for a constant solvent polarity (e.g. in acetonitrile, acn), the smallest clusters with the largest conduction band potentials are capable of driving the electron transfer to both bpy and tmb at faster rates. In fact, the larger D=4.5 nm clusters cannot effectively transfer electrons to tmb,

the more difficult-to-reduce an electron acceptor. We have not shown the D=4.5 nm, tmb ET rates in figure 5 since they are so slow.

Solvent Dependence

Examination of the data of figure 5 shows that reduction of bpy to bpy radical anion is so facile for the smallest $MoS_2$ nanoclusters that solvent polarity has a very minor effect on ET kinetics. For the more difficult to reduce substrate, tmb, the smaller D=3.0 nm clusters show significantly slower ET once the mole fraction of the non-polar solvent, benzene is greater than 0.5. In the case of the D=4.5 nm clusters reducing the solvent polarity slows down the ET dramatically, since lower polarity solvents are less able to stabilize the charge separated state. In fact, effectively no ET to bpy occurs for solvent mixtures of greater than 20 mole% benzene.

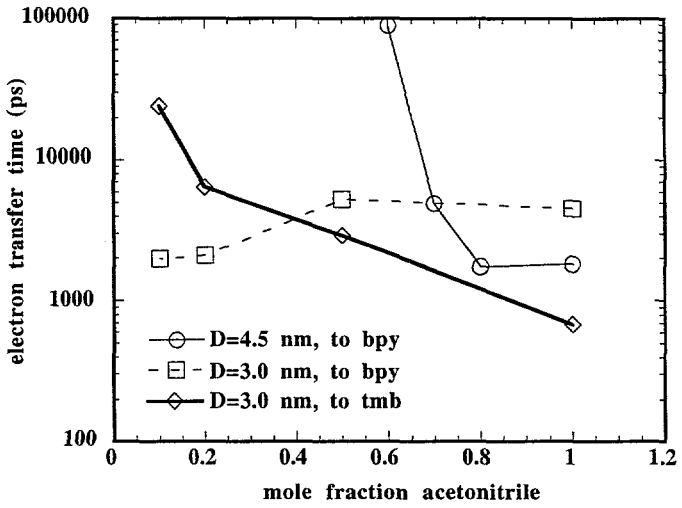


Figure 5. Effect of nanocluster size and solvent in the ET decay times (acetonitrile/benzene mixture).

## CONCLUSIONS

We have shown how quantum confinement in an indirect semiconductor material can shift the conduction band potential and allow facile electron transfer to two types of substrate. Smaller clusters were demonstrated to have improved ET rates. It was also demonstrated that maximizing the solvent polarity increases the ET rate by stabilizing the charge separated state.

## ACKNOWLEDGMENT

This work was supported by the U.S. dept. of Energy under contract DE-AC04-94AL85000. Sandia is a multiprogram lab operated by Sandia Corporation, a Lockheed-Martin Company, for the U.S. Dept. of Energy.

## REFERENCES

[1] J.P. Wilcoxon and G.A. Samara, Physical Rev Rapid Comm. **51**, 7299, (1995).
[2] J.P. Wilcoxon, G. Samara, and P. Newcomer, Proceedings of Symposium F, meeting of the MRS Society, Boston, MA. (1994)
[3] J.P. Wilcoxon, P.P. Newcomer, and G.A. Samara, J. Appl. Phys., submitted, (1996).
[4] B.L. Evans in Optical and Electrical Properties (of Materials with Layered Structures), ed P.A. Lee, D. Reidel Publ, Boston, 1976, Chapt. 1, pg 1.
[5] H. Tributsch, Z. Naturforsch **32a**, 972, (1977).
[6] F. Parsapour, D.F. Kelley, S. Craft, and J.P. Wilcoxon, J. Chem. Phys., **104**, 1, (1996).